Int. J. Electrochem. Sci., 7 **(2012)** 4047 - 4063

International Journal of
ELECTROCHEMICAL
SCIENCE
www.electrochemsci.org

Thermodynamic Characterisation and Density Functional Theory Investigation of 1, 1',5 , 5'-Tetramethyl-1*H*, 1'*H*-3, 3'-Bipyrazole as Corrosion Inhibitor of C38 Steel Corrosion in HCl

H. Zarrok[1], *S. S. Al-Deyab*[2], *A. Zarrouk*[3], *R. Salghi*[4], *B. Hammouti*[3,*], *H. Oudda*[1], *M. Bouachrine*[4], *F. Bentiss*[6]

[1] LPS, Faculté des Sciences, Université Ibn Tofail BP 242, Kénitra, Morocco.
[2] Petrochemical Research Chair, Chemistry Department, College of Science, King Saud University, P.O. Box 2455, Riyadh 11451, Saudi Arabia.
[3] LCAE-URAC18, Faculté des Sciences, Université Mohammed I[er] B.P. 717, 60000 Oujda, Morocco.
[4] EGEB, ENSA, Université Ibn Zohr, BP 1136 Agadir, Morocco.
[4] UMIM, Faculté Polydisciplinaire de Taza, Université Sidi Mohamed Ben Abdellah, Taza, Maroc.
[6] LCCCA, Faculté des Sciences, Université Chouaib Doukkali, B.P. 20, M-24000 El Jadida, Morocco.
[*]E-mail: hammoutib@gmail.com

Received: 15 March 2012 / *Accepted:* 4 April 2012 / *Published:* 1 May 2012

The corrosion inhibition by a 1, 1', 5 ,5'-tetramethyl-1*H*, 1'*H*-3, 3'-bipyrazole (Bip) on C38 steel in hydrochloric acid (HCl) solution has been investigated by weight loss at 308-343K. The results obtained revealed that the inhibition efficiency decreased with increase in temperature. Inhibition occurred through adsorption of the Bip molecules on the metal surface. The value of activation energy (E_a), Arrhenius factor, enthalpy and entropy for the Bip corrosion inhibition and the thermodynamic parameters such as adsorption equilibrium constant (K_{ads}), free energy of adsorption (ΔG°_{ads}), adsorption heat (ΔH°_{ads}) and adsorption entropy (ΔS°_{ads}) values were calculated and discussed. Adsorption of Bip on the C38 steel surface in 1M HCl follows the Langmuir isotherm model. Quantum chemical calculations using DFT at the B3LYP/6-31G* level of theory was further used to calculate some electronic properties of the molecule in order to ascertain any correlation between the inhibitive effect and molecular structure of 1, 1', 5 ,5'-tetramethyl-1*H*, 1'*H*-3, 3'-bipyrazole (Bip).

Keywords: C38 Steel; HCl; Inhibition; Bipyrazole; Weight Loss; Langmuir; DFT

1. INTRODUCTION

Corrosion is a fundamental process playing an important role in economics and safety, particularly for metals and alloys. Steel has found wide application in a broad spectrum of industries

and machinery; however its tendency to corrosion. The corrosion of steel is a fundamental academic and industrial concern that has received a considerable amount of attention. Among several methods used in combating corrosion problems, the use of chemical inhibitors remains the most cost effective and practical method. Therefore, the development of corrosion inhibitors based on organic compounds containing nitrogen, sulphur and oxygen atoms are of growing interest in the field of corrosion and industrial chemistry as corrosion poses serious problem to the service lifetime of alloys used in industry [1-8]. Generally, the corrosion rate of steel in acidic solution increase with the rise of temperature. This is due to the decrease of hydrogen evolution overpotential [2]. Temperatures effects on acidic corrosion, most often in hydrochloric and sulphuric acids, have been the object of a large number of investigations [9–18]. The adsorption of the organic inhibitor at the metal solution interface is the first step in the mechanism of the inhibitory action. Organic molecules may adsorb on the metal surface by

(a) Electrostatic interaction between a negatively charged surfaces, which is provided with specifically adsorbed anions (Cl^-) on metal and positive charge of the inhibitor.

(b) Interaction of unshared electron pair in the inhibitor molecule with metal.

(c) Interaction of π electron of the inhibitor molecule with the metal and/or

(d) A combination of all the above processes.

Adsorption of organic compounds on the metal surface can be described by two types of interaction; physical adsorption and chemical adsorption. Physical adsorption requires the presence of both electrically charged surface in the metal and charged species on the bulk of the solution. Chemisorptions involve charge-transfer process. The object of the present work was to study the temperature effects on C38 steel corrosion in 1 M HCl solution in the absence and presence of various additions of 1, 1', 5 ,5'-tetramethyl-1H, 1'H-3, 3'-bipyrazole (Bip) by using gravimetric method. Various thermodynamic parameters for inhibitor adsorption on C38 steel surface were estimated and discussed. Kinetic parameters for C38 steel corrosion in absence and presence of the studied inhibitor were evaluated and interpreted. On the light of inhibitor constituent, the inhibition mechanism for C38 steel in hydrochloric acid was suggested. The correlation between the inhibition efficiency and quantum chemical parameters was investigated in order to elucidate the inhibition mechanism of the investigated compound. The molecular structure of Bip is shown in Fig. 1.

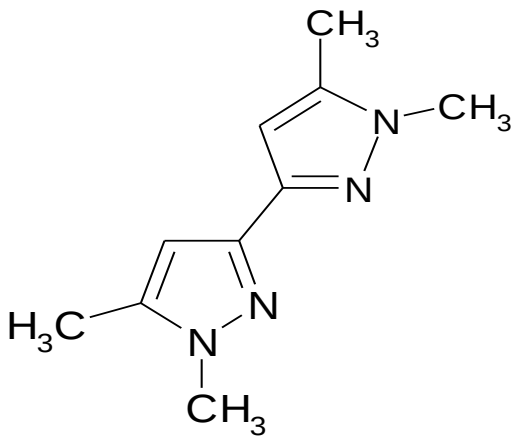

Figure 1. The chemical structure of Bip.

2. EXPERIMENTAL DETAILS

2.1. Materials and reagents

C38 Steel strips containing 0.09 wt.% P; 0.38 wt. % Si; 0.01 wt. % Al; 0.05 wt. % Mn; 0.21 wt. % C; 0.05 wt. % S and the remainder iron were used for gravimetric studies. Prior to all measurements, are abraded with a series of emery paper from 180 to 1200 grade. The specimens are washed thoroughly with bidistilled water degreased and dried with acetone. The specimens are washed thoroughly with bidistilled water degreased and dried with acetone. The aggressive solution (1M HCl) was prepared by dilution of Analytical Grade 37 % HCl with double-distilled water.

2.2. Weight loss measurements

Gravimetric measurements were carried out in a double-walled glass cell equipped with a thermostated cooling condenser. The solution volume was 80 cm^3. Prior to all measurements, the exposed area was mechanically abraded with 180, 320, 800 and 1200 grade emery papers. The specimens were washed thoroughly with bi-distilled water, degreased, and dried with ethanol. The C38 steel specimens used had a rectangular form (1.6cm × 1.6cm × 0.07cm). Three measurements were performed in each case and the mean value of the weight loss was reported and recorded in mg/cm^2. The immersion time for the weight loss was 1 h.

2.3. Quantum chemical calculations

Complete geometrical optimizations of the investigated molecules are performed using DFT (density functional theory) with the Beck's three parameter exchange functional along with the Lee–Yang–Parr nonlocal correlation functional (B3LYP) [19–21] with 6- 31G* basis set is implemented in Gaussian 03 program package [22]. This approach is shown to yield favorable geometries for a wide variety of systems. This basis set gives good geometry optimizations. The geometry structure was optimized under no constraint. The following quantum chemical parameters were calculated from the obtained optimized structure: the energy of the highest occupied molecular orbital (E_{HOMO}), the energy of the lowest unoccupied molecular orbital (E_{LUMO}), $\Delta Egap = E_{HOMO} - E_{LUMO}$, the dipole moment ($\mu$) and total energy (TE).

3. RESULTS AND DISCUSSION

3.1.1. Effect of immersion time

Three parallel rectangular C38 steel specimens of were used for the determination of corrosion rate. The coupons, initial weight using an analytic balance was recorded before immersion in 80 ml of corrodent (1M HCl) without and with different concentrations of Bip. The specimens were taken out,

washed, dried, and reweighed accurately. The average weight loss of the three parallel C38 steel specimens could be obtained. The corrosion rates of have be C38 steel en determined for different immersion period at 308K from mass loss, using Eq. (1) where Δm is the mass loss, S is the area, and t is the immersion period [23]. The percentage protection efficiency $E_w(\%)$ was calculated according the relationship Eq. (2) where W and W_{inh} are the corrosion rates of steel without and with the inhibitor, respectively [24]:

$$W = \frac{\Delta m}{S.t} \quad (1)$$

$$E_w\% = \frac{W - W_{inh}}{W} \quad (2)$$

Fig. 2 shows the effect of increasing time on the weight loss of carbon steel in uninhibited and inhibited acid solutions

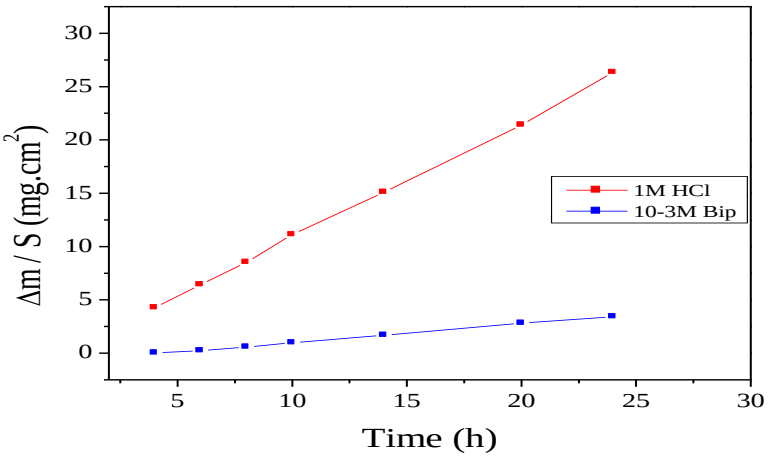

Figure 2. Weight loss as a function of immersion time of steel in 1M HCl without and with 10^{-3}M of Bip at 308 K.

It is obvious that the weight loss varied linearly with immersion period. The curves obtained in presence of the additive fall significantly below that of free acid. The linear variation of weight loss with time in plain acid and inhibited acid indicates the absence of insoluble surface films during corrosion.

3.1.2. Effect of temerature

The influence of temperature on the corrosion behaviour of steel/acid in the presence and absence of the Bip at various concentrations is investigated by weight-loss trend in the temperature rang 308-343K during 1h of immerssion. The collected curves in Fig. 3 show the evolution of corrosion rate (W) with Bip concentration (C) at different temperatures. Fig. 4 indicates that at a given

Bip concentration the corrosion rate of steel increased with temperature. The increase is more pronounced at low concentrations. The results also indicate that for a given temperature, the corrosion rate of steel decreased with increasing inhibitor concentration. The values of inhibition efficiency obtained from the weight loss for different inhibitor concentrations and at various temperatures in 1M HCl are given in Table 1 and Fig. 3.

Is clear that inhibition efficiency increased with increase in inhibitor concentration. The maximum value of inhibition efficiency (E_w%) obtained for 10^{-3}M Bip is 96.3% at 308 K. It shows that inhibition efficiency decreased at higher temperatures. This behavior indicates desorption of inhibitor molecule [25].

Table 1. Corrosion rates and values of Inhibition efficiency (E_w%) from weight loss measurement for steel corrosion in 1M HCl without and with addition of different concentrations of Bip at different temperatures.

Temperature (K)	Concentration (M)	W (mg/cm2.h)	Ew (%)	Θ
	Blank	1.07	-	-
	1×10-3M	0.04	96.3	0.963
308	5×10-4M	0.08	92.5	0.925
	1×10-4M	0.12	88.8	0.888
	5×10-5M	0.19	82.2	0.822
	Blank	1.49	-	-
	1×10-3M	0.07	95.3	0.953
313	5×10-4M	0.13	91.3	0.913
	1×10-4M	0.22	85.2	0.852
	5×10-5M	0.35	76.5	0.765
	Blank	2.87	-	-
	1×10-3M	0.40	86.1	0.861
323	5×10-4M	0.60	79.1	0.791
	1×10-4M	0.86	70.0	0.700
	5×10-5M	1.22	57.5	0.575
	Blank	5.21	-	-
	1×10-3M	1.31	74.9	0.749
333	5×10-4M	1.78	65.9	0.659
	1×10-4M	2.81	46.1	0.461
	5×10-5M	3.56	31.7	0.317
	Blank	10.02	-	-
	1×10-3M	4.29	57.2	0.572
343	5×10-4M	4.92	50.8	0.508
	1×10-4M	6.76	32.5	0.325
	5×10-5M	7.94	20.8	0.208

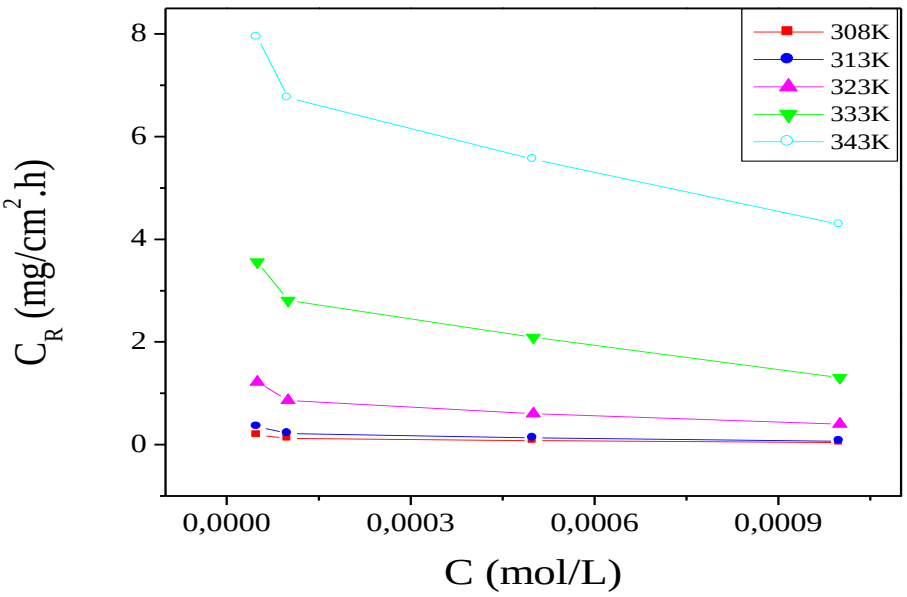

Figure 3. Variation of corrosion rate with the concentrations of Bip for steel in 1M HCl at different temperatures.

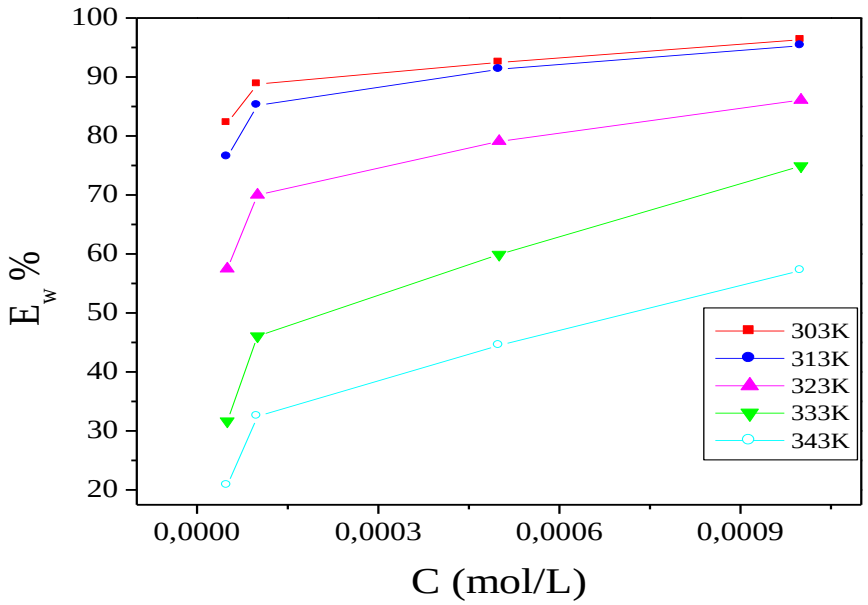

Figure 4. Relationship between inhibition efficiency and concentration of Bip in 1M HCl.

3.1.3. Adsorption isotherm and thermodynamic parameters

The extent of corrosion inhibition depends on the surface conditions and the mode of adsorption of the inhibitors [26]. Under the assumptions that the corrosion of the covered parts of the surface is equal to zero and that corrosion takes place only on the uncovered parts of the surface (i.e., inhibitor efficiency is due mainly to the blocking effect of the adsorbed species), the degree of surface

coverage Θ has been estimated from the chemical and electrochemical techniques employed in this study as follows: $\Theta = E_w$ (%)/100 (Eq. 3) (assuming a direct relationship between surface coverage and inhibition efficiency) [26–29]. The adsorption on the corroding surfaces never reaches the real equilibrium and tends to reach an adsorption steady state. However, when the corrosion rate is sufficiently small, the adsorption steady state has a tendency to become a quasi-equilibrium state.

The adsorption on the corroding surfaces never reaches the real equilibrium and tends to reach an adsorption steady state. However, when the corrosion rate is sufficiently small, the adsorption steady state has a tendency to become a quasi-equilibrium state. In this case, it is reasonable to consider the quasi-equilibrium adsorption in thermodynamic way using the appropriate equilibrium adsorption isotherms [30].

Basic information on the interaction between the inhibitor and the C38 steel surface can be provided by the adsorption isotherm. In order to obtain the isotherm, the linear relation between the values of Θ and the inhibitor concentration (C_{inh}) must be found. Attempts were made to fit the Θ values to various isotherms including Langmuir, Hill de Boer, Parsons, Temkin, Flory–Huggins, Dahar– Flory–Huggins and Bockris–Swinkel. By far the best fit is obtained with Langmuir isotherm. According to this isotherm, Θ is related to C_{inh} by:

$$\frac{\Theta}{1-\Theta} = K_{ads}.C_{inh} \qquad (4)$$

Rearranging Eq. 4 gives:

$$\frac{C_{inh}}{\Theta} = \frac{1}{K_{ads}} + C_{inh} \qquad (5)$$

where K_{ads} is the equilibrium constant of the inhibitor adsorption process, C_{inh} is the inhibitor concentration and Θ is the surface coverage that was calculated by Eq. 3. This model for Langmuir's adsorption isotherm has been used extensively in the literatures for various metal/inhibitor/acid solution systems [31-35].

A fitted straight line is obtained for the plot of C_{inh}/Θ versus C_{inh} with slope close to 1 as seen in Fig. 5. The strong correlation ($R^2 > 0.999$) suggests that the adsorption of inhibitor on the C38 steel surface obeyed this isotherm. This isotherm assumes that the adsorbed molecules occupy only one site and there are no interactions with other adsorbed species [36].

The K_{ads} values can be calculated from the intercept lines on the C_{inh}/Θ-axis. This is related to the standard free energy of adsorption (ΔG°_{ads}) with the following equation 6:

$$\Delta G^{\circ}_{ads} = -RTLn(55.5K_{ads}) \qquad (6)$$

where R is the gas constant and T is the absolute temperature. The constant value of 55.5 is the concentration of water in solution in mol/dm^3 [37].

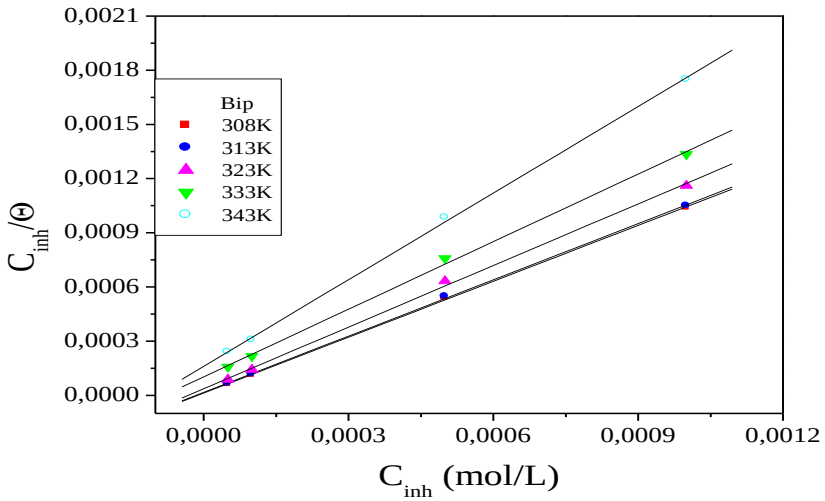

Figure 5. The relationship between C_{inh} / Θ and C of Bip at various temperatures.

Calculated free energies (ΔG°_{ads}) are given in Table 2; the negative values of ΔG°_{ads} indicate spontaneous adsorption of Bip onto the C38 steel surface [38] and strong interactions between inhibitor molecules and the metal surface [39]. Generally, values of ΔG°_{ads} up to -20 kJ mol^{-1} are consistent with physisorption, while those around -40 kJ mol^{-1} or higher are associated with chemisorption as a result of the sharing or transfer of electrons from organic molecules to the metal surface to form a coordinate [40]. In the present study, the estimated ΔG°_{ads} values are lower than -40 $kJ.mol^{-1}$ indicate that the adsorption mechanism of the bipyrazole tested may be a chemisorption. Usually the adsorption free energy involved in a chemisorption process is more negative than 25 kJ/mol [41].

Thermodynamically, ΔG°_{ads} is related to the standard enthalpy and entropy of the adsorption process, ΔH°_{ads} and ΔS°_{ads}, respectively, via Eq. (7):

$$\Delta G^{\circ}_{ads} = \Delta H^{\circ}_{ads} - T\Delta S^{\circ}_{ads} \qquad (7)$$

and the standard enthalpy of adsorption (ΔH°_{ads}) can be calculated according to the van't Hoff equation [42]:

$$\mathrm{Ln}(K_{ads}) = -\frac{\Delta H^{\circ}_{ads}}{\mathrm{R\,T}} + Constant \qquad (8)$$

A plot of Ln K_{ads} versus 1000/T gives a straight line, as shown in Fig. 6. The slope of the straight line is ΔH°_{ads} /R. The value of ΔH°_{ads} is given in Table 2. Since the ΔH°_{ads} value is negative, the adsorption of inhibitor molecules onto the C38 steel surface is an exothermic process. In an exothermic process, chemisorption is distinguished from physisorption by considering the absolute value of ΔH°_{ads}

; for the chemisorption process, it approaches 100 kJ/mol, while for the physisorption process, it is less than 40 kJ /mol [43, 44].

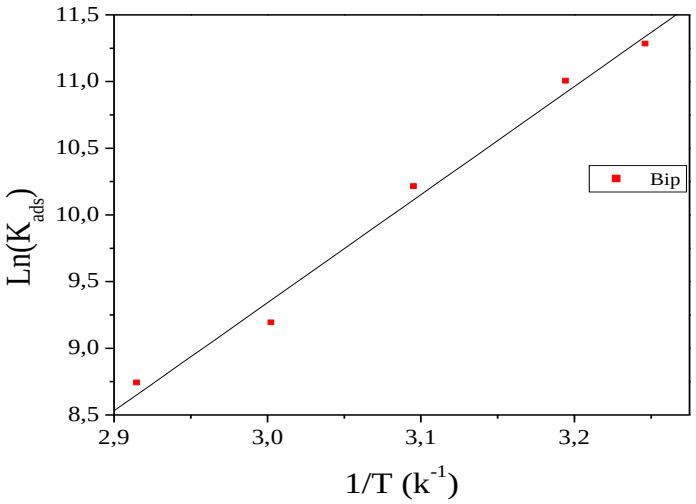

Figure 6. The relationship between Ln(K_{ads}) and 1/T for Bip.

Table 2. The thermodynamic parameters of adsorption of Bip on the steel surface.

T (K)	coefficient de régression Linéaire ®	Kads (L/mol)	ΔG°ads (kJ/mol)	ΔH°ads (kJ/mol)	ΔS°ads (J/mol.K)
308	0.99984	78987.69	-39.162		-91.76
313	0.99985	59797.88	-39.073		-90.58
323	0.99935	27100.19	-38.196	-67.425	-90.49
333	0.99923	9757.24	-36.551		-92.71
343	0.99972	6221.73	-36.365		-90.55

In the present study, the DH0 ads value is larger than the common physical adsorption enthalpy, but smaller than the common chemical adsorption heat, once again emphasizing that both physical and chemical adsorption take place. The same results were obtained by other authors [42, 43, 45, 46]. ΔH°_{ads} = -67.425 kJ mol^{-1} found by the Van't Hoff equation, may be also evaluated by the Gibbs–Helmholtz equation, which is defined as follows :

$$\left[\frac{\partial(\Delta G^{\circ}_{ads}/T)}{\partial T}\right]_P = -\frac{\Delta H^{\circ}_{ads}}{T^2} \qquad (9)$$

Which can be arranged to give the following equation :

$$\frac{\Delta G^{\circ}_{ads}}{T} = \frac{\Delta H^{\circ}_{ads}}{T} + A \qquad (10)$$

The adsorption of inhibitor molecules is accompanied by positive values of ΔS°_{ads}.

Fig. 7 shows the variation of $\Delta G^{\circ}_{ads}/T$ with $1/T$ which gives a straight line with a slope that equals ΔH°_{ads}. It can be seen from the figure that $\Delta G^{\circ}_{ads}/T$ decreases with $1/T$ in a linear fashion. The calculated ΔH°_{ads} using the Gibbs–Helmholtz equation is -67.42486 kJ mol^{-1} for Bip compound, confirming the exothermic behaviour of adsorption on the steel surface, therefore, the values of ΔH°_{ads} obtained by both methods are in good agreement.

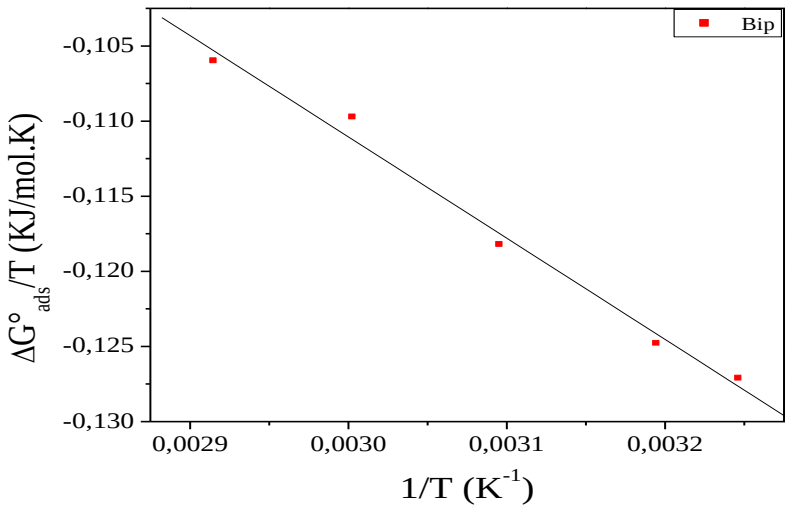

Figure 7. Relationship between ΔG°_{ads}/T and the reverse of absolute temperature.

3.1.4. Corrosion kinetic parameters

The temperature increases the rate of all electrochemical processes and influences adsorption equilibria and kinetics as well. Temperature investigations allow the determination of activation energy, pre-exponential factor and other thermodynamic activation functions in absence and in presence of inhibitor. The activation kinetic parameters such as energy (E_a), enthalpy (ΔH^{*}_{a}) and entropy (ΔS^{*}_{a}) may be evaluated from the effect of temperature temperature using Arrhenius law (Eq. (11)) and the alternative formulation of Arrhenius equation (Eq. (12)) [47]:

$$W = A\exp\left(\frac{-E_a}{RT}\right) \qquad (11)$$

$$W = \frac{RT}{Nh}\exp\left(\frac{\Delta S^{*}_{a}}{R}\right)\exp\left(-\frac{\Delta H^{*}_{a}}{RT}\right) \qquad (12)$$

Where W is the corrosion rate, R the gas constant, T the absolute temperature, A the pre-exponential factor, h the Plank's constant and N is Avogrado's number.

Figs. 8 and 9 show the plots of Ln (W) and Ln (W/T) against 1/T, respectively. Straight lines are obtained with a slope of (ΔH_a^* /R) and an intercept of (Ln R/Nh + ΔS_a^*/R) from which the values of ΔH_a^* and ΔS_a^* are calculated (Table 3).

Literature [47–52] showed that compared with the activation energy in the absence of an inhibitor, higher values for E_a were found in the presence of an inhibitor. Other studies [53, 54] indicated that in the presence of an inhibitor the activation energy was lower than that in its absence. It was clear that (Table 3) the values of E_a in the presence of the Bip are higher than that in the uninhibited acid solution (55.75 kJ mol^{-1}). The decrease of inhibition efficiencies with increasing temperature and the increase of E_a in the presence of the inhibitor indicate the physical adsorption mechanism [55].

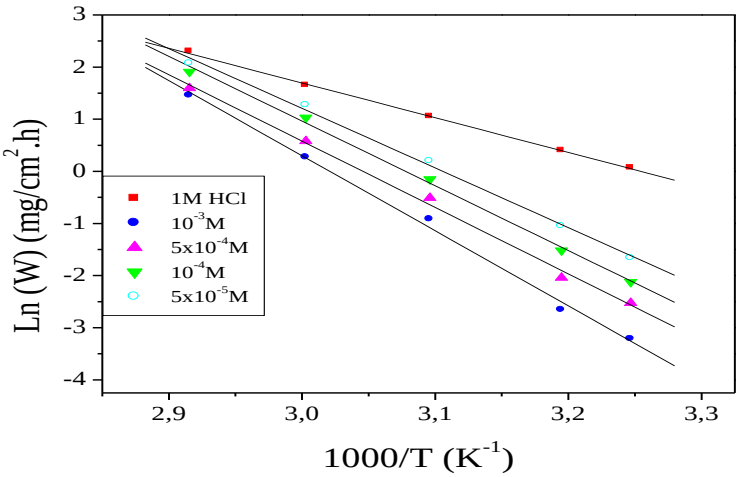

Figure 8. Arrhenius plots of steel in acid with and without different concentrations of Bip.

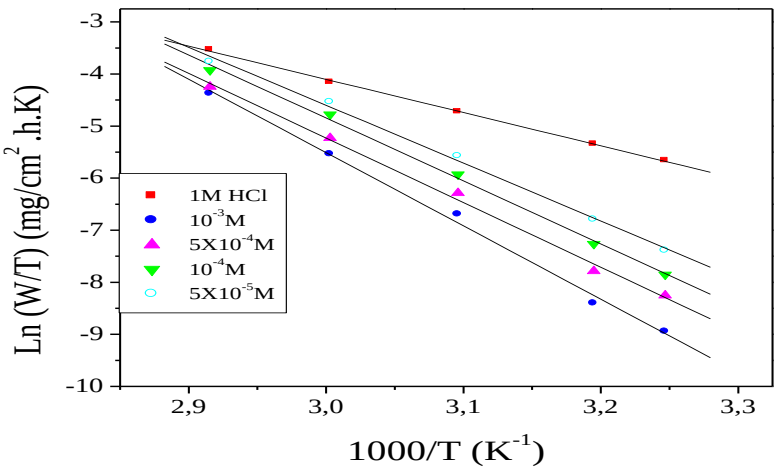

Figure 9. The relationship between Ln (W/T) and T^{-1} for different concentrations of Bip.

The values of ΔH_a^* and E_a are nearly the same and are higher in the presence of the inhibitor. This indicates that the energy barrier of the corrosion reaction increased in the presence of the inhibitor without changing the mechanism of dissolution. The positive values of ΔH_a^* for both corrosion processes with and without the inhibitor reveal the endothermic nature of the steel dissolution process and indicate that the dissolution of steel is difficult [9,56].

The large negative value of ΔS_a^* for C38 steel in 1M HCl implies that the activated complex is the rate-determining step, rather than the dissociation step. In the presence of the inhibitor, the value of ΔS_a^* increases and is generally interpreted as an increase in disorder as the reactants are converted to the activated complexes [9]. The positive values of ΔS_a^* reflect the fact that the adsorption process is accompanied by an increase in entropy, which is the driving force for the adsorption of the inhibitor onto the steel surface.

Fig. 10 indicates that the activation energy increases with the Bip concentration. In the same way, the pre-exponential factor increases with the compound concentration. The variation in pre-exponential factor, as a whole, is just like that of the activation energy. From Eq. (10), it can be seen that at a given temperature, the value of the steel corrosion rate is jointly decided by the activation energy and pre-exponential factor. The steel corrosion rate basically decreases with an increase in concentration of Bip. As can be seen from Table 3, it was clear that both E_a and A increased in the presence of Bip [57].

Table 3. The values of activation parameters for C38 steel in 1M HCl in the absence and the presence of different concentrations of Bip.

Conc (M)	A (mg/cm2.h)	Linear regression coefficient (r)	E_a (kJ/mol)	ΔH_a^* (kJ/mol)	ΔS_a^* (J/mol.K)	$E_a - \Delta H_a^*$ (kJ/mol)
Blank	3.0066×109	0.99961	55.75	53.05	-72.49	2.70
10-3	7.8353×1018	0.99817	119.74	117.04	107.76	2.70
5×10-4	6.9681×1016	0.99820	105.87	103.15	68.50	2.72
10-4	3.9765×1016	0.99861	103.25	100.55	63.83	2.70
5×10-5	2.6893×1015	0.99841	95.11	92.41	41.44	2.70

We remark that E_a and ΔH_a^* values vary in the same way with the inhibitor concentration (Fig. 9 and Table 3). This result permits to verify the known thermodynamic relation between E_a and ΔH_a^* as shown [58]:

$$E_a - \Delta H_a^* = RT \qquad (13)$$

The calculate values are too close to RT is 2.7 kJ/mol. This result shows the inhibitor acted equally on E_a and ΔH_a^*.

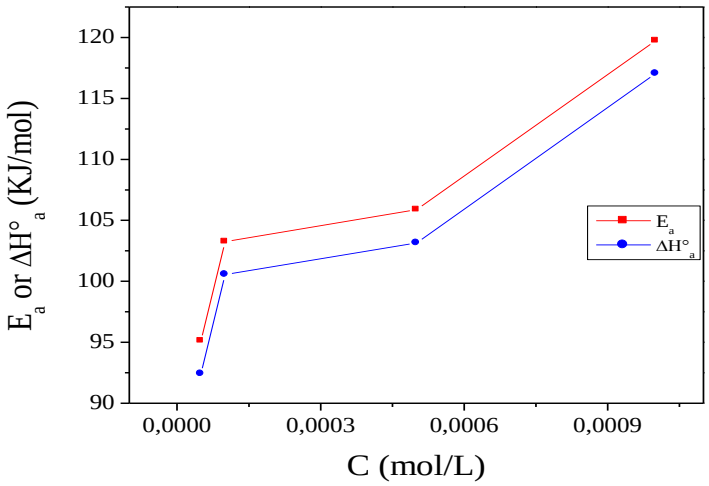

Figure 10. The relationship between E_a and ΔH_a^* with concentration of Bip.

3.6. Quantum chemical calculations

Quantum chemical calculations have been widely used to study reaction mechanisms and have already proven to be very useful in determining molecular structure, electronic structure and reactivity and also for studying corrosion inhibition mechanisms [59]. Thus, it has become a common practice to carry out theoretical calculations in corrosion inhibition studies. The predicted properties of reasonable accuracy can be obtained from density functional theory (DFT) calculations [60, 61]. Some quantum chemical parameters, which influence the electronic interaction between surface atoms and inhibitor, are the energy of highest occupied molecular orbital (E_{HOMO}), the energy of lowest unoccupied molecular orbital (E_{LUMO}), the energy gap E_{HOMO}- E_{LUMO} (ΔE), dipole moment (μ) and total energy (TE). All quantum chemical properties were obtained after geometric optimization with respect to the all nuclear coordinates using Kohn–Sham approach at DFT level. The optimized structure of the studied compound is shown in Fig. 11.

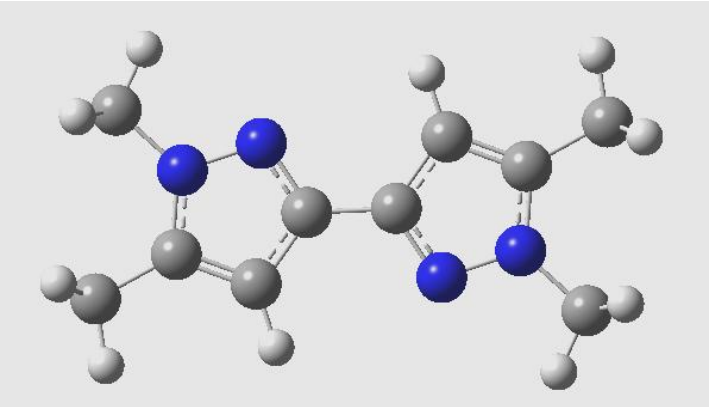

Figure 11. Optimized structure of the studied molecule obtained by B3LYP-6-31 G(d) method.

The computed quantum chemical properties such as energy of highest occupied molecular orbital (E_{HOMO}), energy of lowest unoccupied molecular orbital (E_{LUMO}), HOMO–LUMO energy gap (ΔE_{H-L}), dipole moment (μ) and total energy (TE) are summarized in the Table 4.

Table 4. Calculated quantum chemical parameters of studied inhibitor.

Compound	TE (eV)	EHOMO (eV)	ELUMO (eV)	ΔEgap (eV)	μ (Debye)	ΔN (eV)
Bip	-16429.029	-5.2962	-0.4612	4.8349	0.0000	0.852389

As E_{HOMO} is often associated with the electron donating ability of a molecule, high values of E_{HOMO} are likely to indicate a tendency of the molecule to donate electrons to appropriate acceptor molecules with low-energy, empty molecular orbital. Increasing values of the E_{HOMO} facilitate adsorption (and therefore inhibition) by influencing the transport process through the adsorbed layer. Therefore, the energy of the E_{LUMO} indicates the ability of the molecule to accept electrons; hence these are the acceptor states. The lower the value of E_{LUMO}, the more probable, it is that the molecule would accept electrons [62]. As for the values of ΔE (E_{LUMO} - E_{HOMO}) concern; lower values of the energy difference ΔE will cause higher inhibition efficiency because the energy to remove an electron from the last occupied orbital will be low [63].

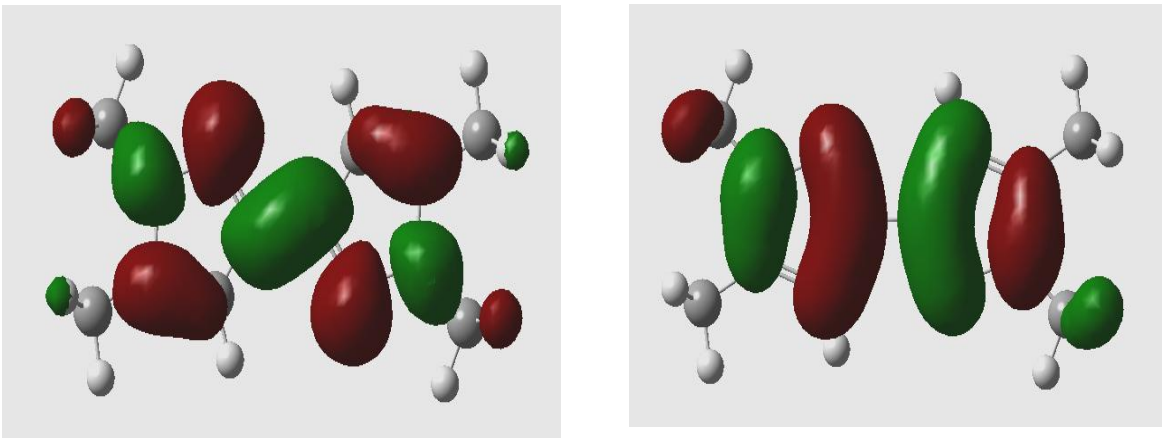

Figure 12. The frontier molecule orbital density distributions of Bip: HOMO (right); LUMO (left).

As we know, frontier orbital theory is useful in predicting the adsorption centers of the inhibitors responsible for the interaction with surface metal atoms. The HOMO and the LUMO population of ATA were plotted and are shown in Fig. 12. Analysis of this figure shows that the densities of LUMO and HOMO were distributed around the entire molecule especially in the aromatic rings. Moreover, the gap between the LUMO and HOMO energy levels of the molecule was another important factor that should be considered. It has been reported that excellent corrosion inhibitors are usually those organic compounds that are not only offer electrons to unoccupied orbital of the metal

but also accept free electrons from the metal [64]. It is also well documented in literature that the higher the HOMO energy of the inhibitor, the greater its ability of offering electrons to unoccupied d-orbital of the metal, and the higher the corrosion inhibition efficiency. It is evident from Table 4 that the studied compound has the highest E_{HOMO} (-5.2962 eV). This confirms the experimental results that interaction between ATA and metal is electrostatic in nature (physisorption). In addition, the lower value of the LUMO energy (-0.4612 eV), the easier the acceptance of electrons from metal surface, as the LUMO-HOMO energy gap decreased and the efficiency of inhibitor improved. Low values of the energy gap (ΔE = 4.83 eV) will provide good inhibition efficiencies, because the excitation energy to remove an electron from the last occupied orbital will be low. The total energy of is equal to -16429.029 eV. This result indicated that Bip molecule is favourably adsorbed through the active centers of adsorption. Lower values of dipole moment (μ) will favour accumulation of the inhibitor in the surface layer and therefore higher inhibition efficiency [65].

4. CONCLUSION

The following conclusions may be drawn from the study:

* Inhibition efficiency increases with the increase of concentration to attain 96.3% at 10^{-3}M.

* Bipyrazole (Bip) acts as an inhibitor for the corrosion of C38 steel in 1 M HCl. Inhibition efficiency values increase with the inhibitor concentration but decrease with rise in temperature suggesting physical adsorption mechanism.

* The adsorption of Bip on steel surface was found to accord with Langmuir adsorption isotherm model. The adsorption process is spontaneous, endothermic and accompanied with a increase in entropy of the system from thermodynamic point of view.

* Kinetic and adsorption parameters were evaluated and discussed.

* Data obtained from quantum chemical calculations using DFT at the B3LYP/6-31G level of theory were correlated to the inhibitive effect of Bipyrazole. Both experimental and theoretical calculations are in excellent agreement.

ACKNOWLEDGEMENTS

Prof S. S. Al-Deyab and Prof B. Hammouti extend their appreciation to Deanship of Scientific Research at King Saud University for funding the work through the research group project.

References

1. A. K. Singh, M. A. Quraishi, *Corros. Sci.* 51 (2009) 2752.
2. A. Popova, E. Sokolova, S. Raisheva, M. Christov, *Corros. Sci.* 45 (2003) 33
3. A. Popova, M. Christov, A. Vasilev, *Corros. Sci.* 49 (2007) 3290
4. M. Lebrini, M. Lagrenee, H. Vezin, L. Gengembre, F. Bentiss, *Corros. Sci.* 47 (2005) 485.

5. H. Zarrok, R. Salghi, A. Zarrouk, B. Hammouti, H. Oudda, Lh. Bazzi, L. Bammou, S. S. Al-Deyab, *Der Pharma Chemica*., 4 (1) (2012) 407.
6. H. Zarrok, H. Oudda, A. El Midaoui, A. Zarrouk, B. Hammouti, M. Ebn Touhami, A. Attayibat, S. Radi, R. Touzani, *Res. Chem. Intermed*., (2012) DOI: 10.1007/s11164-012-0525-x).
7. H. Zarrok, H. Oudda, A. Zarrouk, R. Salghi, B. Hammouti, M. Bouachrine, *Der Pharma Chemica*., 3 (6) (2011) 576.
8. H. Zarrok, R. Saddik, H. Oudda, B. Hammouti, A. El Midaoui, A. Zarrouk, N. Benchat, M. Ebn Touhami, *Der Pharma Chemica*., 3 (5) (2011) 272.
9. I. El Ouali, B. Hammouti, A Aouniti, Y. Ramli, M. Azougagh, E.M. Essassi, M. Bouachrine, *J. Mater. Envir. Sci*. 1 N° 1 (2010) 1.
10. M. Elayyachy, B. Hammouti, A. El Idrissi and A. Aouniti, *Port. Electrochim. Acta*. 29 (2011) 57.
11. M. Benabdellah, A. Tounsi, K.F. Khaled, B. Hammouti, *Arabian J. Chem*. 4 (2011) 17.
12. M. Bouklah, B. Hammouti, M. Lagrene´e, F. Bentiss, *Corros. Sci*. 48 (2006) 2831.
13. M. Bouklah, B. Hammouti, *Port. Electrochim. Acta*. 24 (2006) 457.
14. L. Herrag, B. El Bali, M. Lachkar and B. Hammouti, *Oriental Journal of Chemistry*. 25 (2009) 265.
15. Eno E. Ebenso, Ime B. Obot, *Int. J. Electrochem. Sci*. 5 (2010) 2012 .
16. 16. N.O. Obi-Egbedi, K.E. Essien, I.B. Obot, E.E. Ebenso, *Int. J. Electrochem. Sci*. 6 (2011) 913.
17. M. Benabdellah, K. Tebbji, B. Hammouti, R. Touzani, A. Aouniti, A. Dafali, S. El Kadiri, *Phys. Chem. News*. 43 (2008) 115.
18. N. O. Obi-Egbedi, I. B. Obot, *Corros. Sci*. 53 (2011) 263.
19. A. D. Becke, *J. Chem. Phys*. 96 (1992) 9489.
20. A. D. Becke, *J. Chem. Phys*. 98 (1993) 1372.
21. C. Lee, W. Yang, R.G. Parr, *Phys. ReV. B*. 37 (1988) 785.
22. Gaussian 03, Revision B.01, M. J. Frisch, et al., Gaussian, Inc., Pittsburgh, PA, 2003.
23. A. K. Maayta, N. A. F. Al-Rawashded, *Corros. Sci*. 46 (2004) 1129.
24. K. C. Emreg¨ul, A.A. Akay, O. Atakol, *Mater. Chem. Phys*. 93 (2005) 325.
25. M. Schorr, J. Yahalom, *Corros. Sci*. 12 (1972) 867.
26. M. Christov, A. Popova, *Corros. Sci*. 46 (2004) 1613.
27. F. Bentiss, M. Traisnel, L. Gengembre, M. Lagrenee, *Appl. Surf. Sci*. 152 (1999) 237.
28. B.B. Damaskin, O.A. Petrii, B. Batraktov, Plenum Press, New York, 1971.
29. I. Langmuir, *J. Am. Chem. Soc*. 39 (1917) 1848.
30. R. Alberty, R. Silbey, Physical Chemistry, second ed., Wiley, New York, 1997. p.845.
31. E. A. Noor, A. H. Al-Moubaraki, *Mater. Chem. Phys*. 110 (2008) 145.
32. E. Naderi, A.H. Jafari, M. Ehteshamzadeh, M.G. Hosseini, *Mater. Chem. Phys*. 115 (2009) 852.
33. R. Solmaz, G. Kardas_, M. Culha, B. Yazici, M. Erbil, *Electrochim. Acta*.53 (2008) 5941.
34. E. Machnikova, Kenton H. Whitmire, N. Hackerman, *Electrochim. Acta*.53 (2008) 6024.
35. F. Xu, J. Duan, S. Zhang, B. Hou, *Mater. Lett*. 62 (2008) 4072.
36. Guls_en Avci, *Colloids and Surfaces A: Physicochemical and Engineering Aspects* 317 (2008) 730.
37. O. Olivares, N. V. Likhanova, B. Gomez, J. Navarrete, M. E. Llanos-Serrano, E. Arce, J. M. Hallen, *Appl. Surf. Sci*. 252 (2006) 2894.
38. L. Tang, X. Li, L. Lin, G. Mu, G. Liu, *Mater. Chem. Phys*. 97 (2006) 301.
39. Z. Sibel, P. Dogan, B. Yazici, *Corros. Rev*. 23 (2005) 217.
40. G. Moretti, F. Guidi, G. Grion, *Corros. Sci*. 46 (2004) 387.
41. E. Geler, D.S. Azambuja, *Corros. Sci*. 42 (2000) 631.
42. L. B. Tang, G. N. Mu, G. H. Liu, *Corros. Sci*.,45 (2003) 2251.
43. M. Benabdellah, R. Touzani, A. Dafali, M. Hammouti, S. El Kadiri, *Mater. Lett*. 61 (2007) 1197.
44. E. A. Noor, A. H. Al-Moubaraki, *Mater. Chem. Phys*. 110 (2008) 145.
45. E.A. Noor, A.H. Al-Moubaraki, *Corros. Sci*. 51 (2009) 868.

46. X. Li, G. Mu, *Appl. Surf. Sci*. 252 (2005) 1254.
47. S. T. Arab, E. A. Noor, *Corrosion*., 49 (1993) 122.
48. M. Elachouri, M. S. Hajji, M. Salem, S. Kertit, J. Aride, R. Coudert, E. Essassi, *Corrosion*., 52 (1996) 103.
49. E.S. Ferreira, C. Giacomelli, F.C. Giacomelli, A. Spinelli, *Mater. Chem. Phys*. 83 (2004) 129.
50. A. Zarrouk, I. Warad, B. Hammouti, A. Dafali, S.S. Al-Deyab, N. Benchat, *Int. J. Electrochem. Sci*. 5 (2010) 1516.
51. B. Hammouti, A. Zarrouk, S. S. Al-Deyab and I. Warad, *Oriental Journal of Chemistry*., 27 (2011) 23.
52. A. Zarrouk, B. Hammouti, H. Zarrok, S. S. Al-Deyab, M. Messali, *Int. J. Electrochem. Sci.* 6, (2011) 6261.
53. S. N. Banerjee, S. Misra, *Corrosion*., 45 (1989) 780.
54. Q. H. Cai, Y. K. Shan, B. Lu, X. H. Yuan, *Corrosion*., 49 (1993) 486.
55. A. Popova, E. Sokolova, S. Raicheva,M. Christov, *Corros. Sci*. 45 (2003) 33.
56. G.N. Mu, X.M. Li, F. Li, *Mater. Chem. Phys*. 86 (2004) 59.
57. M. Behpour, S.M. Ghoreishi, N. Soltani, M. Salavati-Niasari, M. Hamadanian, A. Gandomi, *Corros. Sci*. 50 (2008) 2172.
58. M. Stern, A. L. Geary, *J. Electrochem. Soc*. 104 (1957) 56.
59. E. Kraka, D. Cremer, Computer design of anticancer drugs, *J. Am. Chem. Soc*. 122 (2000) 8245.
60. C. Adamo, V. Barone, *Chem. Phys. Lett*. 330 (2000) 152.
61. M. Parac, S. Grimme, *J. Phys. Chem. A*. 106 (2003) 6844.
62. G. Gece, *Corros. Sci*. 50 (2008) 2981.
63. R.M. Issa, M.K. Awad, F.M. Atlam, *Appl. Surf. Sci*. 255 (2008) 2433.
64. P. Choa, Q. Liang, Y. Li, *Appl. Surf. Sci*. 252 (2005) 1596.
65. N. Khalil, *Electrochim. Acta*. 48 (2003) 2635.